Bird Velocity Optimization as Inspiration for Unmanned Aerial Vehicles in Urban Environments

Cara J. Williamson,* Anouk Spelt,† and Shane P. Windsor‡
University of Bristol, Bristol, England BS8 1TR, United Kingdom

https://doi.org/10.2514/1.J059438

Small unmanned aerial vehicles (SUAVs) operating in urban environments must deal with complex wind flows and endurance limitations caused by current battery technology. Birds offer inspiration regarding how to fly in these environments and how to exploit complex wind flows as an energy source. On a broad scale, migrating birds adjust airspeed to minimize cost of transport (COT) in response to wind conditions, but it is unknown whether birds implement these strategies in fine-scale, complex environments. GPS backpacks were used to track 11 urban nesting gulls and found they soared extensively during daily commutes, using thermal and orographic updrafts. This paper outlines COT theory and proposes a model for optimizing airspeed for wind while maintaining flight trajectory. The gull flight paths were tested for COT adjustments, considering their flapping and soaring strategies, and it was found that the birds were able to make energy savings of 31% based on having a best glide speed when soaring that was similar to their minimum power speed when flapping. These models calculated optimum airspeeds based on wind speed and direction and could be implemented on SUAV platforms with wind sensing capabilities. This approach could significantly reduce energy requirements for SUAVs flying in urban environments.

Nomenclature

D	=	aerodynamic drag force, N
E	=	energetic cost, J
e	=	velocity tracking error, m/s
g	=	acceleration due to gravity, m/s^2
$h_{AGL,HAS}$	=	altitude above ground level, height above structure, m
$k_{f,s}$	=	drag factor in flapping or soaring flight
m	=	body mass, kg
r	=	flight range, m
$S_{b,w}$	=	surface areas of body or wing, m^2
U	=	velocity in air frame, m/s
$U_{bg,mp,mr,ms}$	=	best glide, minimum power, maximum range, and minimum sink velocities, m/s
V	=	velocity in inertial frame, m/s
V_z	=	sink speed in inertial frame, m/s
W	=	wind speed, m/s
$W_{a_{h,s}}$	=	head- or side-wind component in air frame, m/s
θ_D	=	wind direction, deg
$W_{i_{h,c}}$	=	head- or cross-wind component in inertial frame, m/s
W_z	=	vertical wind component, m/s
$\beta_{a,i}$	=	angle between velocity and wind vectors in air or inertial frame, deg
ϕ_i	=	heading in inertial frame, deg

I. Introduction

SMALL unmanned air vehicles (SUAVs) have the potential to fly at low altitudes within the urban environment, making them suitable for a range of missions such as infrastructure monitoring, surveillance, emergency response, and small payload delivery [1–5]. However, current SUAVs have two main technology limitations. First, SUAVs have limited capacity to cope with the high levels of turbulence and complex flows created by wind interactions within the urban landscape [6–8]. Second, due to the power–constraints in battery technology, SUAVs have a limited range and endurance [9,10]. This research takes a novel approach to finding ways of overcoming these limitations by looking at the ways birds make use of wind flows in the urban environment to reduce their energetic cost of flight.

Birds of comparable size and weight to small SUAVs are able to navigate the complex city wind flows and exploit these environments to reduce the energetic cost of flight. During the breeding season, urban gulls spend up to 40% [11] of their time in flight, flying to and from foraging locations through these complex windscapes. Choosing appropriate flight strategies has the potential to substantially reduce their energetic flight costs and could be key for breeding success. Understanding the energy saving strategies urban gulls are using to reduce flight costs can inspire approaches to extend the range and endurance of SUAVs flying in similar environments.

Flight mechanics theory shows that transport costs can be minimized by adjusting airspeed with relation to wind conditions. In unfavorable conditions such as headwinds, airspeed should be increased, and in favorable conditions such as tailwinds, airspeed should be reduced. Vertical wind components also effect transport costs; a downdraft will increase the cost of transport (COT), and therefore airspeed should be increased, and an updraft will reduce COT, and so airspeed should be decreased. Gull species studied in migration and in long-range open water commutes have been found to make velocity and even altitude adjustments to headwinds that act to maximize COT savings [12,13]. However, these flights tend to experience uniform and predictable flow conditions which are not representative of the urban environment.

A recent study found that urban gulls spend up to 10% more time in flight than those in traditional habitats [11], so it may be that the complex flows generated by our architecture creates more soaring opportunities than are available in more traditional habitats. Certainly, studying gulls in this environment can provide new insight into managing these complex flows. Previous work found that gulls exploit the wind highways generated by urban terrain [14], and a SUAV flight control strategy based on the gulls flight behavior achieved a throttle reduction of 15% while minimizing overall control effort [15]. Additional SUAV studies have found that exploiting urban flow can successfully be used to gain significant altitude [16] and that choosing the correct airspeed and climb angles for the wind gradient can be used to make savings of 12% in the field [10]. Certainly then, studying birds in urban environments can present

Presented as Paper 2020-1948 at the AIAA SciTech 2020, Orlando, FL, January 6–10, 2020; received 17 January 2020; revision received 26 August 2020; accepted for publication 28 October 2020; published online 3 June 2021.

*Research Associate, Department of Aerospace Engineering.
†Ph.D. Candidate, Department of Aerospace Engineering.
‡Senior Lecturer, Department of Aerospace Engineering.

strategies which are advantageous to SUAV technology. However, there has been little research in the way birds use wind flows in the urban environment and whether velocity adaptions for COT are common for all wind conditions.

This study aims to discern whether COT velocity adaptions are advantageous when implemented in the complex flow conditions created by urban infrastructure using commuting urban gulls as a case study. First, we outline relevant flight mechanics theories regarding velocity optimization before detailing a velocity optimization algorithm suitable for use when flying on a fixed heading with knowledge of current wind conditions. Following this, the methods used for capturing and analyzing flight data from GPS tagged gulls are described, including how the data were downselected and categorized into different soaring strategies. The velocity optimization models are then tested against the different flight strategies employed by the gulls to determine their potential for energy savings in urban environments.

II. Flight Models

This section contains the flight mechanics theory behind the velocity optimization models used throughout. The glide polar and mechanical power curve models used for the gulls are outlined along with the key velocities involved with optimizing flight performance. An explanation of COT theory follows, where the relationship between airspeed and the wind conditions is introduced. This relationship is used to outline an algorithm for calculating the optimum airspeed for a fixed trajectory and known wind conditions. Three potential flight speed selection models for flapping flight are then introduced.

A. Velocity Curves

Avian flight has typically been studied at two very different scales. At one end of the spectrum, the precise mechanics and aerodynamics of flight has been studied in controlled environments such as wind tunnels, which has given rise to detailed models used to predict flapping power requirements [17–19] and optimum glide ratios [20–23], while on the broad scale, flight mechanics models have been used to study the energy saving techniques implemented by migratory birds in relation to weather systems [12,13,24–26].

Probably the most widely used glide polar model for birds was developed by Pennycuick [27] and popularized by the Flight software. This method calculates glider polars using the same methods as for fixed-wing aircraft, separating the induced aerodynamic drag force from the viscous drag generated by the friction over the wings and body. A power curve approach is then used to model flapping flight, with the induced drag being considered proportional to the absolute minimum power required to stay in flight, calculated by modeling the moving wings as an actuated disk [27].

The drag forces in flight vary with velocity in a manner which results in minima in both the glide polar and the power curve (Fig. 1). These minima represent the lowest rate of energy exchange, which in flapping flight is the minimum power output and in gliding flight is the minimum sink rate; the velocities at which these occur will be referred to as the minimum power U_{mp} and minimum sink U_{ms} velocities respectively. Flying at these airspeeds will result in maximum flight endurance but will not result in the lowest energy cost for a given distance. The lowest energy cost for transport can be found at the tangential to each of the curves (Fig. 1e) and is referred to as maximum range velocity U_{mr} for flapping flight and best glide velocity U_{bg} for gliding flight. These velocities for the average lesser black-backed gulls, *Larus fuscus*, used in this study are summarized in Table 1.

The glide polar and power curve models were generated using equations and aerodynamic characteristics from Pennycuick's [27] 2008 model and collected gull biometrics (Table 2).

B. Cost of Transport Theory

When flying through moving air, it is important to consider the effect of the wind on relative motion. The energetic cost required to travel a given distance can vary significantly depending on the direction and velocity of the wind flow. For example, progress in the inertial frame is impeded when flying at a set airspeed in a headwind compared to still air, which increases the duration and cost of flight. The velocity reference frames can be seen in Fig. 1 and are related by Eq. (1), where V is the ground speed, U is the airspeed, and W is the wind speed.

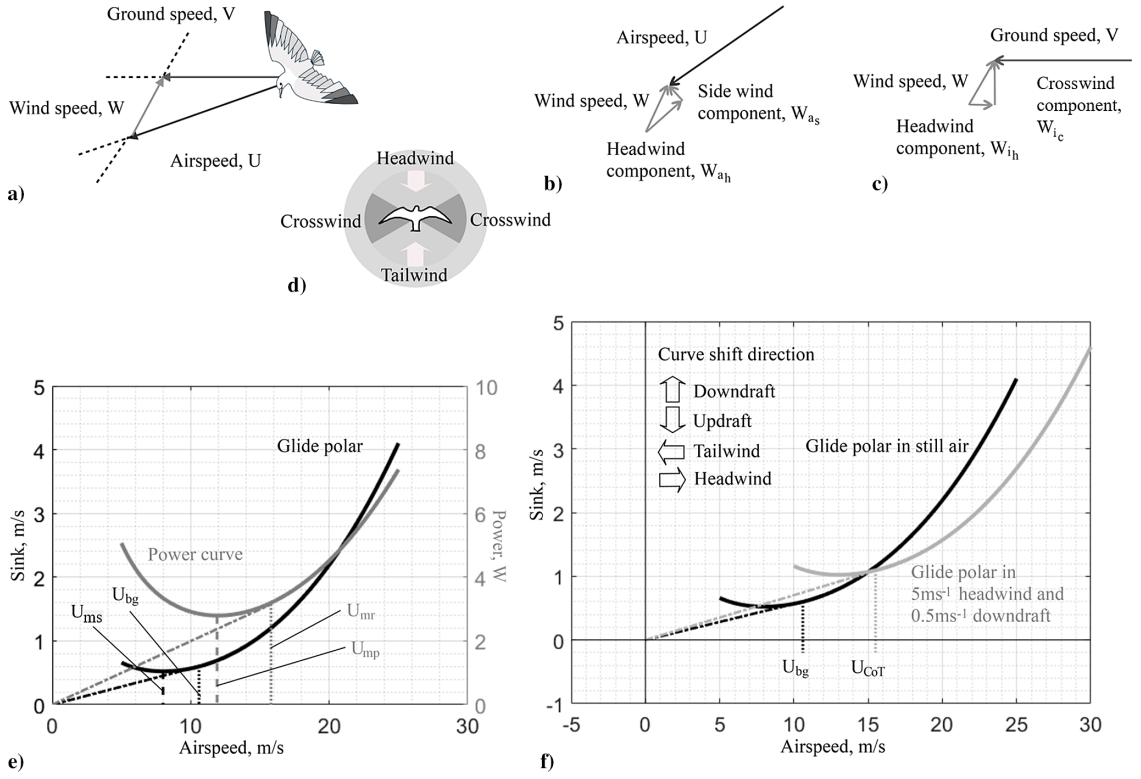

Fig. 1 Velocity diagrams and plots for calculating: a) airspeed, b) head wind in the air frame, c) headwind in the inertial frame, d) headwind [±(0° – 60°)], crosswind ±(60° – 120°) and tailwind ±(120° – 180°) angles, e) glide polar and power curve, f) COT curve shifting.

Table 1 Performance airspeeds for flapping and gliding flight for the average gull

Velocity name	Symbol	Airspeed, m/s	Optimization
	Flapping		
Minimum power	U_{mp}	11.9	Endurance
Maximum range	U_{mr}	15.4	Range
	Gliding		
Minimum sink	U_{ms}	8.2	Endurance
Best glide	U_{bg}	10.6	Range

$$U = V - W \tag{1}$$

Many studies have derived the necessary velocity changes required in order to minimize flight cost [27–30]. In a recent study, Taylor et al [30], derived Eq. (2), which considered the cost of transport in the air reference frame (Fig. 1b). The cost of transport or the energy cost E, for a given range r, is considered in terms of the thrust requirements to overcome drag for a given airspeed DU minus the effect of any weight supporting vertical wind. The wind conditions, where W_{a_h} and W_{a_s} are the head- and side-wind components, also have an effect. In summary, the equation shows that COT is reduced by updrafts ($W_z > 0$) or tailwinds ($W_{a_h} < 0$) and increased in downdrafts ($W_z < 0$) or headwinds ($W_h > 0$),

$$-\frac{dE}{dr} \approx \frac{DU - mgW_z}{\sqrt{(U - W_{a_h})^2 + W_{a_s}}} \tag{2}$$

It should be noted that wind vectors, composed of head and side winds, can be considered in two ways aligning with reference to the air frame (Fig. 1b) or the inertial frame (Fig. 1c). COT is calculated for a given distance and so could be considered in the inertial frame [31]; however, in environmental harvesting strategies, it is the airspeed in relation to the wind which should be optimized [30]. This study considers the wind vectors in the air and inertial frame as side and crosswinds, respectively.

In gliding flight, if the updraft is greater than the minimum sink rate, the COT optimization can break down, as flying at a faster speed can still decrease the COT. In this case, it is possible to fly at a speed which matches the sink rate on the glide polar. This is particularly relevant to glider pilots using thermals to fly long distances where gliding between thermals is moderated based on the thermal updraft strength. For glider pilots, the theory is best known as speed to fly (STF), or MacCready's theory [28], where the overall flight time is optimized and considers the time in and between thermals to calculate an overall cross-country speed. Calculating the new optimum airspeed in both STF and COT can be achieved by shifting the glide polar for the experienced conditions as depicted in Fig. 1f. An updraft shifts the curve toward the x axis, and in COT theory, the optimized velocity tends to the minimum sink velocity until the updraft is equal to the minimum sink. In STF theory, the thermal strength can be much greater than the minimum sink value, and here the optimized velocity increases with thermal strength.

Gulls soaring using orographic lift have been found to position themselves such that sink is offset and altitude maintained rather than to benefit from increasing velocity [14], suggesting that they follow COT during orographic soaring. However, several soaring species of bird have been found to follow MacCready's STF in interthermal glides, so this was also tested [32–34].

C. Velocity Optimization Algorithm

This section details a velocity optimization algorithm that can be used to generate the optimum airspeed for COT minimization when flying on a fixed heading with knowledge of current wind conditions. An iterative process was used to calculate the optimum airspeed and resultant ground speed; this considered that as the airspeed changed the relative wind direction also changed as the gull adjusted air relative heading to compensate for slip and maintain inertial heading.

The trajectory holding assumption follows that daily commuting flight, lasting between 10–30 min, is long enough for the bird to want to reduce energy costs but short enough that using wind drift will not provide any total benefit. Additionally, many of these commutes exhibit orographic soaring behavior in which following a ridge feature is vital to continue energy harvesting. This is also applicable for SUAV technology where holding a fixed trajectory is part of the mission plan:

1) Start with the nonadjusted optimum velocity, for example, U_{bg} for gliding flight. Calculate the angle between the wind and ground speed vector β_i given the trajectory heading θ, wind speed W, and direction W_D:

$$\beta_i = \arcsin(W/U_{bg}) \sin(\theta_D - \phi_i) \tag{3}$$

2) Calculate the air relative wind direction β_a:

$$\beta_a = 180 - ((\theta_D - \phi_i) + \beta_i) \tag{4}$$

3) Calculate the air relative headwind W_{a_h}:

$$W_{a_h} = W \cos \beta_a \tag{5}$$

4) Shift the glide polar or power curve, as shown in Fig. 1f, by the headwind component calculated in the previous step and any vertical wind component, resulting in a new airspeed U_{opt}. This step can also be achieved using a look-up table as described in [30].

5) Calculate the new resultant ground speed V using the assumption that the gulls are trajectory holding and that there is no slip:

$$V = \sqrt{(U_{\text{opt}}^2 + W^2 - 2U_{\text{opt}} W \cos \beta_a)} \tag{6}$$

6) Repeat with new air and ground speeds (holding trajectory heading, wind speed, and wind direction constant), until the error e between the start and end airspeeds calculated for the loop is less than $0.1\ \text{m} \cdot \text{s}^{-1}$:

$$e = |U_{\text{opt}} - U| \tag{7}$$

D. Velocity Test Models

The velocity optimization models use the glide polar and power curves generated by the aerodynamic characteristics from Pennycuick's [27] 2008 model and the gulls biometrics in Table 2. A fixed-wing variation of the glide polar model was used due to the sufficient similarity at airspeeds of less than 16 m/s (accounting for 69% of the data) to other methods which include span reduction. Optimized velocity was calculated by shifting the glide polar by the airspeed and/or vertical wind and a new tangent calculated as described in Fig. 1e. The power curve model for flapping flight was also generated using sampled gull biometrics and values from Pennycuick's 2008 Flight model with a drag factor k of 1.1 being used. The Pennycuick model predicts that gulls fly at minimum power velocity due to power constraints in the pectoral muscles [27]; however, some literature

Table 2 Wing and body biometrics

Statistic	Span, m	Mass,kg	Wing area, m^2	Aspect ratio	Chord, m	Frontal area, m^2
Mean, μ	1.15	0.741	0.168	7.85	0.146	0.0067
Standard deviation, σ	0.065	0.061	0.018	0.63	0.011	0.00036

suggests that this would mean no airspeed optimizations are then required [13]. To test these theories, we selected three models:

1) Model 1 is flying at minimum power speed but maintaining flight time. This model uses U_{mp} as the optimum velocity but shifts airspeed only if there is a headwind. There is no adjustment from U_{mp} in tailwinds. The adjusted velocity is the minimum of the headwind shifted curve.

2) Model 2 is flying at minimum power speed with no attempt at airspeed optimization, the only change being the effect of wind on the ground speed.

3) Model 3 is matching flight speed to COT optimized best glide velocity U_{bg} during both gliding and flapping flight.

III. Methods

This section includes details of the experimental data capture and processing. The gull tracking, details of environmental data sets, flight-path filtering, and the classification of soaring strategies are presented.

A. Bird Tagging

This research analyzed the flight paths of 11 lesser black-backed gulls, *Larus fuscus*, tracked using GPS backpacks [35] over two breeding seasons in the city of Bristol, England. All work was approved by the University of Bristol Animal Welfare and Ethical Review Body (UIN: UB/15/069). Bird handling and tagging was conducted under British Trust for Ornithology (BTO) permit A/2831, additional details can be found in [11]. Biometrics for the individuals were recorded at the time of capture and used to characterize the morphology of an average individual (Table 2).

B. Biologging Data

The GPS loggers collected spatial fixes containing latitude, longitude, altitude, and a date–time stamp, with each fix being immediately followed by a 1 s burst of 20 Hz three-axis accelerometer data. The spatial data were used to reconstruct the flight paths of the gulls, and the acceleration data were used to classify flight behavior at each position. Details of the behavior classification can be found in [11,36]. This study used four of these behavior classes (Fig. 2): extreme flapping (such as in takeoff and landing), flapping, soaring, and mixed (combination of soaring and flapping).

A spatial fence trigger was used to adjust the GPS capture frequency of the tags. When the gulls were on their nest, the capture rate was set to a GPS fix every 10 min (600 s). The devices were programmed to increase frequency to a minimum of every 5 min (300 s) after leaving the nest area, defined by a radius of 50 m. The tags were charged by solar panels, and when the tag had a sufficiently high battery voltage, the tag switched to a high-frequency data capture rate of every 4 s. The commuting flights data set required high-frequency recordings, preferably at the high-voltage tag setting of 4 s intervals. As a result of the GPS fence, the outbound flights recorded have a low temporal resolution for the first 5–10 min before switching to the higher 4 s frequency.

C. State Variables

State variables associated with the flights such as velocity, altitude, and heading were calculated as follows. The ground speed of the gulls at the time of data capture was considered to be the instantaneous speed as calculated by satellite Doppler shift, as opposed to point-to-point differencing. Vertical and horizontal ground speeds were calculated separately in the case of gliding flight in order to compare forward and sink speeds. The altitude above sea level (ASL) was calculated using the GPS measured altitude. The altitude above ground level (AGL) and altitude above structure (HAS) were calculated using a digital elevation model from 2 m resolution Light Detection and Ranging (LIDAR) data surface models [37]. The AGL is calculated as the ASL minus the digital terrain model height, whereas the HAS is calculated as ASL minus the digital surface model height and filtered for noise with a 5 m threshold. Heading and directional change angles were calculated using the latitude and longitude captured by the tags with a Haversine transformation adjusted for latitude at the nest location and accurate to 1%, which was considered accurate enough for the short point-to-point distances calculated.

D. Commuting Flights

Commuting flights were defined as nonstop flights between frequently visited locations. These flights were chosen under the assumption that the individuals were not foraging nor searching but traveling between known locations and, as such, more likely to be conserving energy. The full data set was filtered to include only flights to and from 72 locations based on repeated visits. The locations were found using a combination of observation and spatial clustering of terrestrial location fixes. The commuting flights were defined using the filter criteria:

1) A series of flight behavior data points enclosed by two terrestrial fixes at takeoff and landing.

2) A direct flight between takeoff and landing locations with no additional stops (terrestrial points).

3) The Start and end locations were not the same.

4) A flight must have ten or more fixes per kilometer flown, ensuring that trajectory resolution is suitably high.

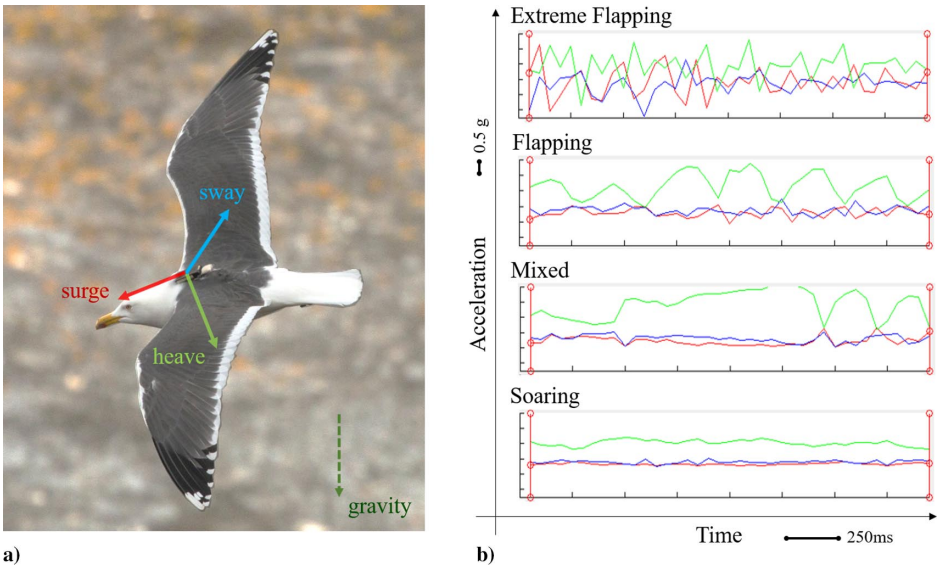

Fig. 2 Surge, heave and sway forces as recorded by the GPS tags a) shows axis position when fitted on a lesser black-backed gull b) examples of triaxial accelerometer data recorded four flight behaviors: extreme flapping, flapping, mixed and soaring.

5) A flight must have more than ten total fixes to ensure that flights are suitably long for evaluation.

6) The flight must be repeated on four occasions such that there is a comparison set.

7) Flights with obvious detours, foraging, or loitering were removed.

8) The Start and end locations were at least 2 km apart.

This resulted in a set of 192 flights ranging between 2 and 20 km, with $\mu = 6.3$ km, $\sigma = 3.5$ km.

E. Weather Data

The weather data used in this study were sampled from the output of the high-resolution United Kingdom variable forecasting model. The forecasting model had a spatial resolution of 2 km and a temporal resolution of 1 h and had the highest resolution of any available data set over the United Kingdom [38]. Each GPS fix was assigned to the nearest 1 h time prediction and then spatially interpolated. The wind speed and direction were interpolated for altitude and used to calculate airspeed. The forecast data were validated using data from a two week period of data collected by two locally situated weather stations: one at the nest site and a second close to the area where the majority of gull foraging occurred. The Pearson product–moment correlation coefficients computed for wind speed ($R = 0.87$, $n > 120{,}000$, Root Mean Square Error, RMSE $= 1.87$ m/s) and wind direction ($R = 0.81$, $n > 120{,}000$, RMSE $= 33.6$ deg) showed that forecasting model gave wind estimates in good agreement with those measured directly.

F. Soaring Strategies

Data points were given an additional flight mode classification based on the soaring strategies used. All data points previously classified as soaring behavior were further categorized into soaring strategies: gliding (with subsets high and low altitude), thermaling, orographic, and other using a decision tree classifier (Fig. 3) with examples in Fig. 4 (background courtesy of Google Earth [39]):

1) Gliding is unpowered flight where gravitational and kinetic energies are traded. Here, it was defined as soaring behavior with a sink rate (downward vertical velocity) greater than 0.55 m/s. This was selected as the minimum sink rate from the glide polar (Fig. 1e). Classification of gliding was performed on the first branch of the decision tree (Fig. 3). In some analysis, gliding was further classified by altitude. High-altitude gliding such as between thermals (Fig. 4a) was classified by the same altitude threshold as the second branch in the decision tree. Low-altitude gliding was defined as below this threshold and occurred between sections of flapping, mixed, or orographic soaring modes.

2) In thermal soaring, altitude is gained by circling in columns of warm rising air, as shown in Fig. 4a. This was characterized first by high-altitude flight where both altitude above ground level h_{AGL} and height above surface structure h_{HAS} were considered. Second, by a high variance in flight direction $\sigma(\phi_i)$ and a consistent heading change $\Delta\phi_i$ of 30° or greater between fixes, shown by the final lower branch of the decision tree (Fig. 3).

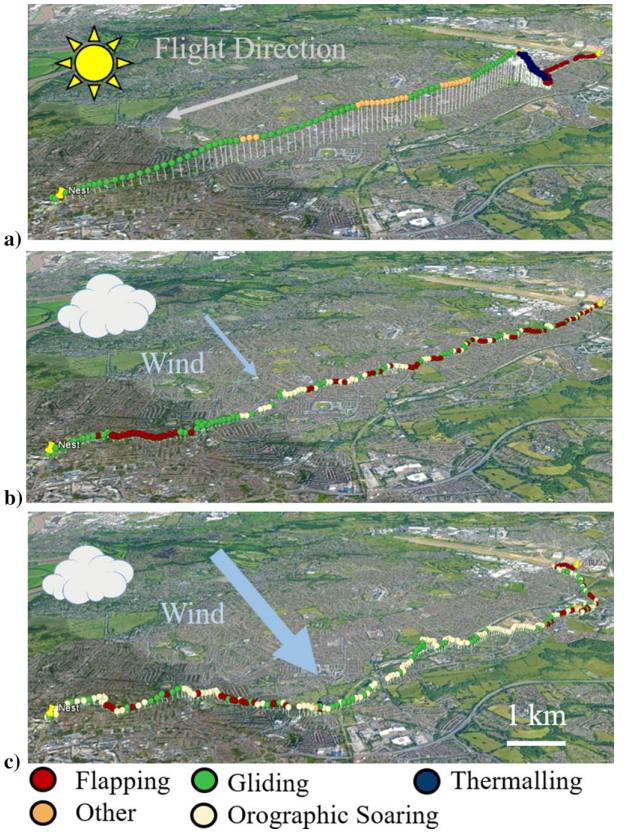

Fig. 4 Flights from one individual occurring with three different weather conditions: a) high thermal availability, overcast with westerly wind; b) 2.75 m/s; and c) 7.72 m/s.

3) Orographic soaring uses updrafts generated on the windward side of a terrain feature, such as a cliff, hill, or building, to offset sink in gliding flight. It requires a relatively low altitude to be within range of any updrafts. Examples of orographic soaring can be seen in Figs. 4b and 4c. The strategy was classified when the circling and altitude measures were below given thresholds, as seen in the upper final branch of the decision tree (Fig. 3).

4) The *other* class contains any soaring behavior which did not fall into the previous categories. This class contained a small fraction of low-altitude thermaling, or circling in areas of very strong orographic lift, see examples in Fig. 4c, but mostly contained high-altitude soaring with no directional variance. This was most likely travel

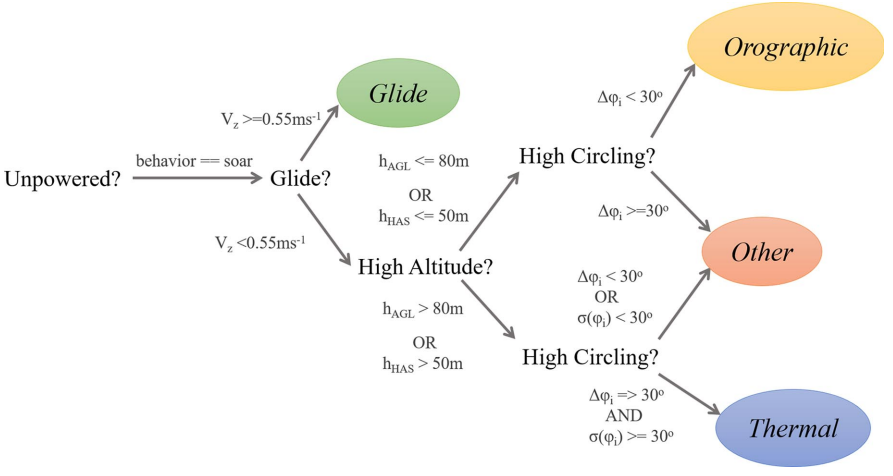

Fig. 3 Flight strategy decision tree: first branch filters behavior, second branch filters using vertical speed, third branch sorts by altitude, and final branch sorts trajectory directionality.

through unexploited thermals or detached thermal bubbles, an example of which is shown in Fig. 4a.

Soaring strategy classification was validated with three methods: first, by expert comparison with a set of ten selected flights across the range of soaring strategies; second, using a systematic variation of the threshold values to check for classification robustness; and, third, by using a machine learning classification model trained with algorithm classified data and input variables from a geophysical, meteorological, and time of day data set as found in [14]. Specifically, thermal and orographic flight strategies were tested as these strategies occurred in different conditions. The Classification Learner toolbox in MATLAB® 2018a was used with a medium grain, k-clustering algorithm and a fivefold test-train ratio. The classification of thermal and orographic points was found to agree with the decision tree algorithm with a 95% accuracy.

G. Interthermal Gliding

Interthermal gliding was examined by finding thermal and glide pairs that fell within three criteria: first, there must be five or more consecutive thermal points in the initial and subsequent thermals; second, the glide section joining the two thermal sections contains more than 50% gliding strategy data with a low directional variance; and, third, all thermal-glide data must be high-frequency data. All commuting flights were searched for thermal-glide pairs giving a total of 19 high-quality thermal-glide pairs. The thermal climb rate was calculated as the average vertical velocity, and the interthermal velocity was calculated as the average airspeed over the entire glide sequence between thermals.

IV. Results

A. Time Budgets and Soaring Strategies

When flying in urban areas, the gulls were able to make extensive use of environmental energy, soaring 30% of the time (Fig. 5b). This increased to 44% when just commuting flight was considered (Fig. 5c). The gulls used a mix of different gliding and soaring strategies (Fig. 5d), the most common combination being thermal soaring followed by sections of high-altitude gliding and occasional soaring (labeled *other*) through updraft pockets such as thermal bubbles. On days with low thermal availability but some wind, orographic soaring was used extensively in combination with low-altitude gliding and mixed flight.

The high amount of thermal soaring behavior measured suggests that the urban environment provides a significant level of thermal availability. Commuting flights that used thermaling were recorded with high percentages of nonflapping flight, with some flights containing as much as 100% soaring flight. These flights also contained soaring consistent with passing through thermals or thermal bubbles without circling to gain altitude and without the need to deviate significantly from the shortest commuting path, suggesting there was a greater number of thermals available than required.

The urban environment offered soaring opportunities when there was little or no thermal availability. These flights contained a mix of orographic soaring, low-altitude gliding, and mixed flight and on average contained a higher fraction of flapping flight than thermaling flights. Flights featuring orographic soaring also featured higher levels of mixed behavior, with some flights featuring as much as 60% soaring flight and 40% mixed, and no flapping flight. It was expected that orographic updraft availability would be higher on days with stronger winds and as such these conditions would feature a higher percentage of orographic soaring. However, orographic soaring showed only a small increase with wind speed compared to a significant decrease in the proportion of flapping flight and an increase in the proportion of mixed flight. The percentage of orographic soaring increased with relation to the wind speed with a positive Pearson correlation ($R = 0.19$, $n = 2623$, $p < 0.001$), suggesting the gulls were able to make use of orographic updrafts across a range of wind speeds. The percentage of flapping was found to decrease with increasing wind speed with a negative correlation ($R = -0.34$, $n = 11{,}285$, $p < 0.001$). The relatively low correlation could be explained by an absence of flapping flight on days with low wind speeds and high thermal availability. Mixed flight, however, was found to increase with wind speed with a strong positive correlation ($R = 0.64$, $n = 5829$, $p < 0.001$). Overall, these changes in behavior in relation to wind speed indicates that the gulls were able to make use of the higher environmental energy available on windy days but may have had higher control demands as represented by the higher level of mixed maneuvering flight.

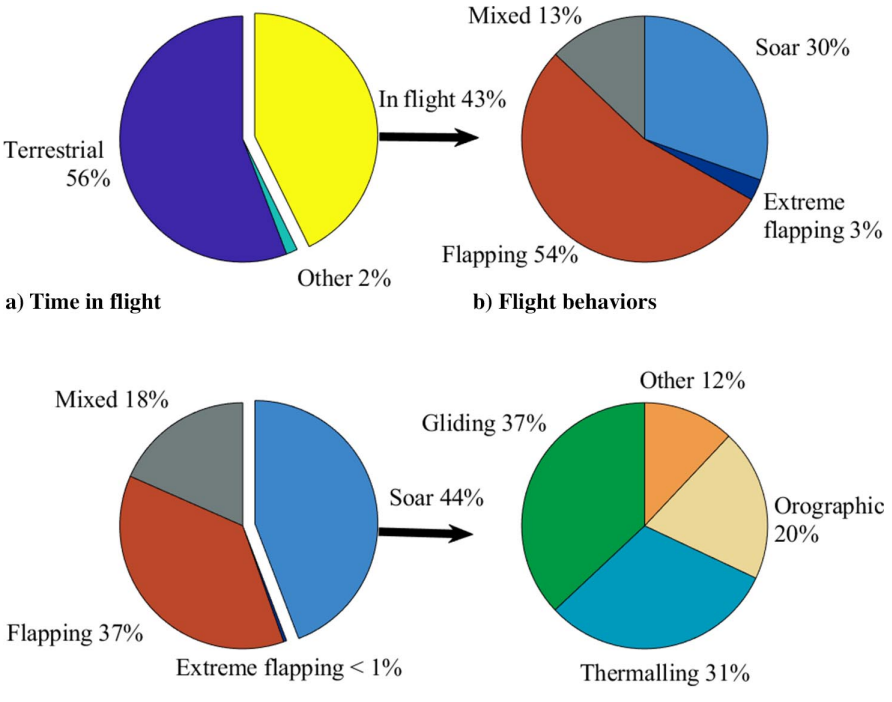

Fig. 5 Time budgets for a) terrestrial and in-flight behavior, b) all flight behaviors, c) commuting flights behaviors, and d) commuting flights soaring strategies (all gliding grouped).

Table 3 Airspeeds for flight behaviors and soaring strategies

Flight type	Mean	Standard deviation	ANOVA	
	μ, m/s	σ, m/s	f value	p value
		Flight behaviors		
Flap	11.4	3.7	$f_{\text{flap–soar}} = 0.95$	0.33
Soar	11.9	4.4	$f_{\text{soar–mix}} = 134,$	< 0.001
Mixed	12.7	4.6	$f_{\text{flap–mix}} = 176,$	< 0.001
		Soar strategies		
Thermal	9.6	3.7	$f_{\text{therm–flap}} = 1870$	< 0.001
			$f_{\text{therm–soar}} = 1091$	< 0.001
Orographic	10.9	3.8	$f_{\text{oro–flap}} = 75$	< 0.001
			$f_{\text{oro–soar}} = 62$	< 0.001
Other	12.3	4.6	$f_{\text{oth–flap}} = 26$	< 0.001
			$f_{\text{oth–soar}} = 32$	< 0.001
Gliding (all)	13.8	4.5	$f_{\text{glide–flap}} = 20$	< 0.001
			$f_{\text{glide–soar}} = 26$	< 0.001
Gliding (low altitude)	11.7	3.2	$f_{\text{low–flap}} = 2493$	< 0.001
			$f_{\text{low–soar}} = 1786$	< 0.001
Gliding (high altitude)	14.8	4.7	$f_{\text{high–flap}} = 2074$	< 0.001
			$f_{\text{high–soar}} = 992$	< 0.001

B. Airspeeds of Flight Behaviors and Soar Strategies

The gulls were found to have different airspeeds depending on their flight behavior or soaring strategy (Table 3). In flapping and soaring flight, the gulls flew slightly slower than the predicted minimum power, $U_{\text{mp}} = 11.9\ \text{m} \cdot \text{s}^{-1}$, and best glide, $U_{\text{bg}} = 10.6\ \text{m} \cdot \text{s}^{-1}$, velocities, respectively. The mixed flight average airspeed was considerably higher and could be associated with gusts and fast corrective maneuvres. Unexpectedly, the average velocity in soaring flight was slightly higher than that in flapping flight; however, the difference was not significant.

The altitudes flown by the gulls varied from 0 to 923 m (AGL), where the median altitude flown on nonthermaling days was 34 m. When thermaling, the gulls thermaled to a mean maximum altitude of over 600 m. Because of the altitude ranges, equivalent airspeeds are used, where the gulls' airspeeds were calculated using the air density ratio at altitude to standard atmospheric pressure. When soaring strategies were compared using an analysis of variance test (ANOVA), all the airspeed distributions were found to be statistically different from flapping flight ($p < 0.001$) and each other ($p < 0.001$), apart from the cases of other to mixed flight with significance of $p < 0.05$ and other to low-altitude gliding which was not significantly different ($p = 0.98$) from soar. Where a strategy has been tested against soaring behavior, the strategy has been removed from the soar data set; for example, orographic soaring was tested against all the soaring behavior flight points that were not classified as orographic soaring. Interestingly, high-altitude gliding, such as between thermals, was faster than the low-altitude gliding, such as between intermittent flapping or orographic soaring ($f_{\text{high–low}} = 619$, $p < 0.001$). Thermaling flight, indicated in Fig. 6 in blue, had the lowest average velocity at 9.6 m/s and was close to the minimum sink velocity at 8.2 m/s, which would provide good altitude gain but was still fast enough to have a safety margin for avoiding stall. During orographic soaring, the average airspeed was 10.9 m/s, close to the best glide velocity for soaring flight, at 10.6 m/s. The average gliding airspeed was much higher at 13.8 m/s and was significantly higher than the best glide velocity ($p < 0.001$).

C. Airspeed Optimization in Soaring Strategies

The gulls used different airspeed adaptions in relation to the relative wind direction depending on the soaring strategy being used. The relationships between airspeed and the air relative wind direction are plotted for four soaring strategies (Fig. 7) and demonstrate the different airspeed adaptions used in each strategy. In Fig. 7, the central line in each plot is the optimum COT airspeed for a 6 m/s wind with no updraft, the upper line is the optimum with an added

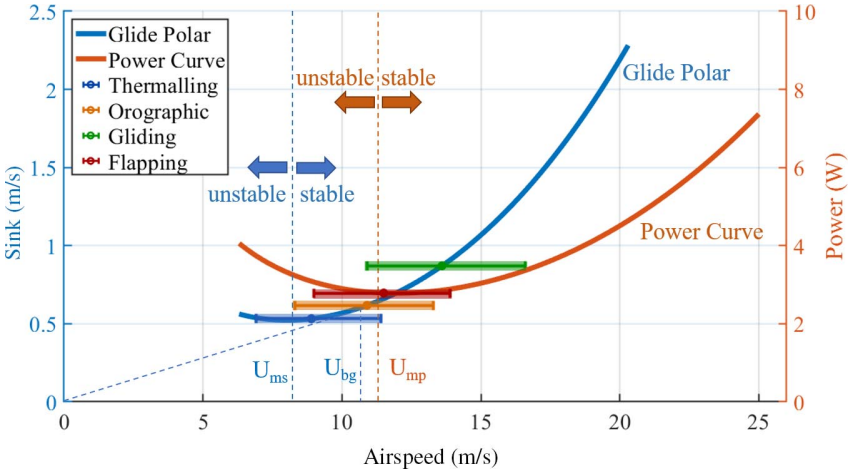

Fig. 6 The airspeeds of four flight strategies; thermaling (blue), orographic (yellow), gliding (green), and flapping (red), are indicated with the mean and standard deviation highlighted by the dot and wings respectively. Bars are plotted over the glide polar (thermaling, orographic and gliding) and power curve (flapping).

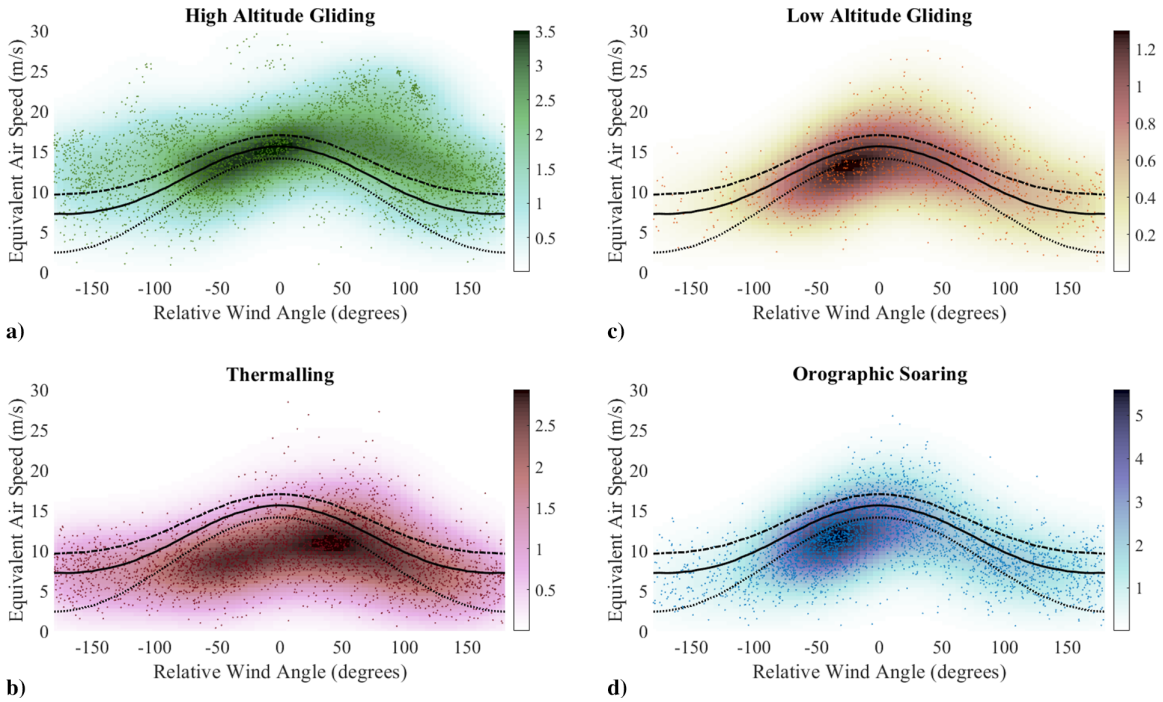

Fig. 7 Equivalent airspeeds at the relative wind direction compared to COT model: a) high-altitude gliding flight, b) thermal soaring, c) low-altitude gliding flight, and d) orographic soaring.

downdraft of −0.5 m/s, and the lower line is the optimum for an added updraft of 0.5 m/s. The data shown are for wind speeds between 4.5 and 7.5 m/s. A Gaussian filter is used alongside the gull data to demonstrate density.

In high-altitude gliding, the gulls made the expected adjustments for the wind direction but flew slightly faster than expected (Fig. 7a), as shown by the data following the shape of the curve but with many points higher than the predicted COT optimum. In thermaling flight, the gulls made relatively little adjustment to their airspeed for the relative wind direction (Fig. 7b), as shown by their consistent airspeed across all relative wind directions. The gulls did make adjustments for the wind direction during low-altitude gliding and orographic soaring (Fig. 7c and 7d), and it can be seen that the gulls followed the predicted model except around a relative wind direction of 50 deg. This angle corresponds to a crosswind in the inertial frame and would occur when flying along a terrain feature perpendicular to the wind. Here, the gulls flew slower than predicted by the COT model. A similar pattern was also seen in the data at lower (less than 4.6 m/s and higher (greater than 7.5 m/s) wind speeds, and orographic soaring behavior occurred at a wind speed average 5 m/s (mean ± s.d. = 5.08 ± 1.71 m/s).

The airspeed data and model both used the measured wind conditions in their calculations, which could introduce false correlation. To show that this did not affect the reliability of the model, ground speed predictions are also compared with the direct velocity measurements of the gulls (Appendix A) and showed that the results were consistent using either airspeed or ground speed.

D. Interthermaling

During high-altitude gliding, the gulls flew faster than the best glide velocity, so it was expected that the gulls would fly at an airspeed described by MacCready's STF theory, shown as a dashed line in Fig. 8. However, the results show that the gulls flew slower than the optimum cross-country speed, as shown by the 19 interthermal flights indicated by the filled markers. A second model using headwind adjustments and thermal strength is shown with square markers and also overpredicts the flight speeds. Modeling the airspeed using COT adjustments for horizontal wind is indicated by the crosses and gave a closer approximation to the measured gull airspeeds. Thermal updraft speeds were not measured directly but were estimated by considering the thermal climb rate of the gulls

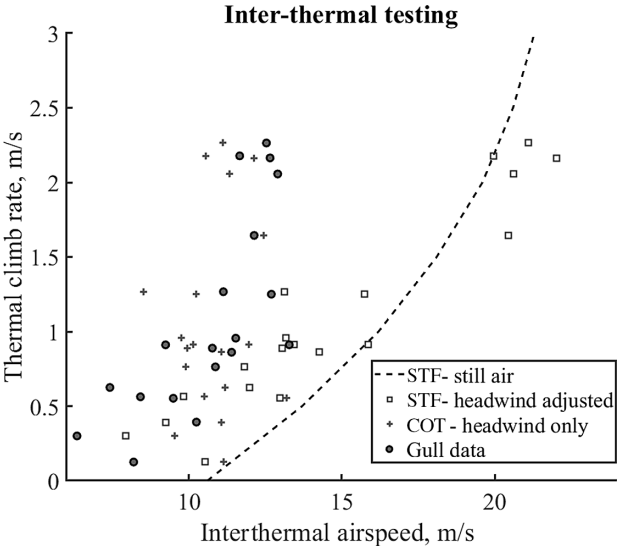

Fig. 8 STF and COT models compared with 19 interthermaling flights.

(plotted in Fig. 8) plus the sink rate corresponding to the average airspeed of the gull while thermaling, giving a mean and standard deviation of 1.62 ± 0.67 m/s.

E. Flapping Flight and Wind Direction

During flapping flight, the gulls appear to fly at their best glide speed modified for the relative wind direction according to COT theory, as represented by model 3 colored green in Fig. 9. The mean ground speed predicted by adjusting best glide velocity for the head- and crosswinds conditions experienced by the gulls was a close match to the flight speeds recorded, while the model slightly underestimated the ground speeds flown by the gulls during a tailwind. Using a model which adjusted minimum power airspeed to maintain minimum flight duration (model 1 shown in white) produced an overestimate of ground speeds for headwinds and crosswinds and also underestimated the ground speed in tailwinds. Meanwhile, maintaining minimum power velocity regardless of the wind

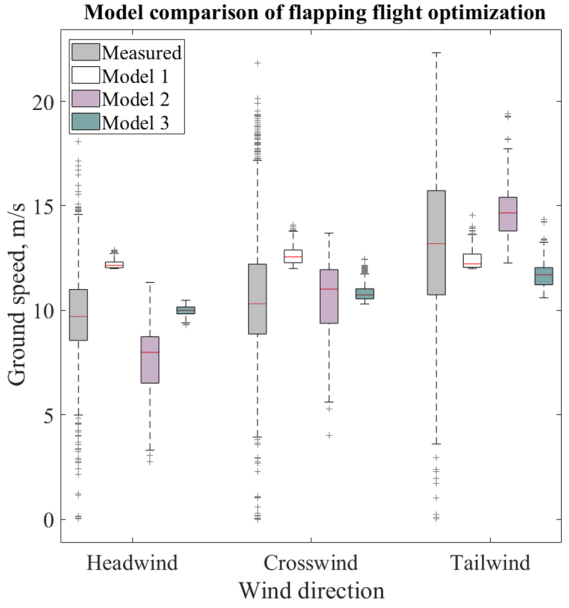

Fig. 9 GPS ground speeds compared against models. M1: optimizing U_{mp} and headwind shifting; M2: maintaining U_{mp} regardless of headwind; and M3: matching U_{bg} and headwind shifting.

conditions (model 2 shown in pink) produced a good estimate of ground speed in crosswinds but underestimated in headwinds and overestimated in tailwinds.

The gulls minimum power velocity is only slightly above their best glide velocity. This means that transitioning from soaring flight to flapping flight can be done efficiently without requiring a large power output for acceleration. This suggests that flapping at a velocity close to the best glide speed could be advantageous in complex flow environments where updrafts are readily available. This could facilitate energy harvesting where the mechanical power requirements at the mean airspeed for head- and tailwinds correspond to only a +6% rise from the minimum power requirement, as seen in Table 4. The average airspeeds, shown in Table 4, indicate that during orographic soaring the gulls slow down in cross- and tailwinds, which both offer favourable COT conditions. In gliding flight, the gulls airspeeds are higher, indicating either an absence of updrafts or that the birds are not exploiting them.

V. Discussion

With the increase in SUAV technology, the fine-scale flight strategies of birds offers inspiration for improved methods of energy harvesting. Implementation of avian soaring strategies on SUAV technology has the potential to greatly increase both endurance and range performance which would otherwise be restricted by the relatively low onboard power capacity. However, studies in this area are often performed via simulation [15,40–42] or in comparatively simple flow conditions [10,34]. This study considers that urban nesting gulls could offer valuable insight into the flight strategies suitable for the complex flow environment generated by city landscapes.

We tracked the flights of 11 urban nesting gulls using GPS loggers, which allowed the measurement of their position, velocity, and behavior. The gulls were able to extensively harvest environmental energy during their daily commutes using a combination of different soaring strategies to exploit thermal and orographic updrafts. Building materials, such as concrete and asphalt, cause urban heat island effects [43,44] so it follows that an abundance of these materials also generates high levels of thermal updrafts that these gulls were seen to exploit. Additionally, gulls have been shown to use man-made infrastructure for orographic soaring in coastal areas where the buildings act as artificial cliffs [14], and this study indicates that this can be extrapolated over cities where the urban canyons create a network of wind highways for soaring. Clearly, the combination of thermal and orographic updrafts provides a large source of environmental energy within urban areas available for harvesting in soaring flight and suggests that SUAVs designed with soaring capabilities could be able to drastically reduce their flight costs during urban missions, given the right control schemes.

A. Soaring Strategies

The gulls used different strategies and airspeeds to harvest energy from different environmental sources. We found that the gulls made use of thermal updrafts combined with high-altitude gliding. In thermaling flight, their airspeed remained close to their minimum sink velocity regardless of wind direction. Using a low airspeed promotes maximum altitude gains by requiring the lowest sink offset.

Table 4 Mean airspeeds for wind conditions

Statistic	Wind direction		
	Headwind	Crosswind	Tailwind
	Flap		
Mean airspeed μ, m/s	14.8	11.8	9.2
Power at mean airspeed, W	3.0, (+6%)	2.8, (U_{mp})	3.0, (+6%)
Standard deviation σ, m/s	3.2	2.8	3.1
Sample size n	3408	5417	2460
ANOVA f values	$f_{head-cross} = 1184$	$f_{cross-tail} = 1856$	$f_{tail-head} = 4769$
ANOVA p values	< 0.001	< 0.001	< 0.001
	Orographic		
Mean airspeed μ, m/s	14.2	11.0	7.4
Standard deviation σ, m/s	2.9	2.5	2.7
Sample size n	916	1199	508
ANOVA f values	$f_{head-cross} = 658$	$f_{cross-tail} = 633$	$f_{tail-head} = 1935$
ANOVA p values	< 0.001	< 0.001	< 0.001
	Gliding (low altitude)		
Mean airspeed μ, m/s	15.3	12.5	9.6
Standard deviation σ, m/s	3.3	3.4	3.8
Sample size n	584	1058	731
ANOVA f values	$f_{head-cross} = 221$	$f_{cross-tail} = 314$	$f_{tail-head} = 901$
ANOVA p values	< 0.001	< 0.001	< 0.001

In gliding flight, the minimum sink and stall speeds are extremely close; the minimum sink speed lies at the boundary of the unstable velocity region where a small decrease in velocity could result in deceleration to the stall speed [27,45]. Flying with a small safety margin above the minimum sink alleviates risk, which is particularly important when flying in crowded thermals [46]. Glider pilots and other bird species have also been found to make this same risk-mitigating compromise [33,34,47]. From the data we collected, we estimated thermal updrafts used by the gulls had a mean updraft of 1.62 m/s but have not ascertained whether the gulls selected thermals, or areas within thermals, with these updraft speeds intentionally or whether they were limited by another factor such as turn radius. It is possible that urban thermals could provide a much greater range of updraft speeds; the center of thermals in particular tend to have the highest updraft speed, which could mean that a SUAV with a smaller turn radius may gain altitude at a faster rate.

When gliding between thermals, the gulls made use of COT optimization for horizontal winds, and although results indicate that there may be some velocity adjustment for updraft, the gulls did not fly at the high speeds predicted by STF. It is possible that the gulls did not perform STF due to an apparent abundance of thermals. The gulls were also seen performing straight soaring, nonflapping, flight between thermals consistent with flying through a thermal or thermal bubble [48] but not circling. Flying at a glide speed slightly above the best glide could mean the gulls are able to make use of the updrafts without overly extending their flight time. This could be particularly relevant during the chick-rearing period where time away from the nest could impact breeding success. Interestingly, a recent simulation study optimizing the velocity of UAVs in interthermal flight [49] found evidence which could support this theory. The study found that interthermal flight was optimal at a velocity between the best glide and STF velocities. The best glide velocity optimizes for the energy cost per distance, whereas the STF predicted velocity provides the overall best flight speed when considering the time required to gain altitude. For the gulls, this suggests that, while COT is an important factor, that time away from the nest could also be an important driver.

The gulls were also able to perform high levels of soaring flight during periods of low thermal availability. In these cases, they performed a combination of flapping, gliding, and orographic soaring flight. The orographic soaring analysis showed that the gulls flew slower than expected when making COT adjustments for headwinds alone, indicating that the gulls are making use of orographic updrafts available in the city. Other bird species have also been found to reduce airspeed in orographic soaring when compared to straight gliding [32], further supporting the gulls' exploitation of orographic lift. We found orographic soaring occurred over a range of wind speeds reaching up to 9.5 m/s; however, interquartile range spanned 3.86–6.27 m/s, although this range could be a reflection of the prevailing wind conditions for the area. The airspeeds flown by the gulls followed the pattern of adapting for COT and supports previous findings where it was discovered that gulls varied spatial position within the orographic updraft field in order to occupy a narrow band of the available updraft suitable for offsetting the sink associated with speeds close to the best glide velocity [14]. Surprisingly, the orographic soaring was not limited to wind directions consistent with soaring in parallel to ridge features. Flying with a tailwind over terrain features provides updrafts on the windward side of the feature, followed by a section of downdraft on the leeward side. Gulls flying perpendicularly over buildings could use the updraft on the windward side to gain altitude for clearance over the building. This could explain the large range of velocities measured when flying in tailwinds and suggests gulls or SUAVs should slow down through the updraft on the windward side of buildings and speed up through the leeward downdraft to harvest as much energy as possible.

B. Wing Morphology

Wing morphology has a profound effect on the gulls' velocity envelope. Gulls have a relatively low wing loading like many soaring birds, but when compared to other marine bird species (such as the albatross), they have a lower aspect ratio. The low wing loading results in being able to circle in narrow thermals but means a lower cross-country speed [32]. The gulls have a much lower wing loading (44 N/m^2) than that of manned gliders (>80 N/m^2) and some other thermaling bird species [32,34]. Perhaps the gulls' low wing loading influences the cross-country speeds more than predicted by the STF model. We explored the wing loading constraints on velocity by comparing the flown airspeeds against a velocity envelope generated using Federal Aviation Regulation (FAR) 23.333 regulations for light aircraft [50] and found that the maximum airspeed for a gull-sized platform would be 21 m/s (Appendix B), a speed that would be reserved only for extreme maneuvre cases. While the low wing loading of the gulls may limit their glide speed, their wing aspect ratio could have, in part, contributed to their success in urban environments. A relatively low aspect ratio results in greater wing-beat power [32], which could be beneficial to the gulls in three ways. First is by facilitating ground based takeoffs. Second is by assisting in high-powered maneuvres that could be required when navigating around obstacles. Third is in the extreme flapping behavior as seen during foraging [11]. However, the aspect ratio of the gull wing is no doubt a tradeoff between having a high aspect ratio wing for good glide performance and a lower aspect ratio wing for lower power requirements in flapping flight.

C. Energy Savings

The birds' flight speeds measured during orographic soaring, low-altitude gliding, and flapping flight are very similar, suggesting that matching flapping speed to the soaring speed could have energy saving benefits. In flapping flight alone, the energetically cheapest speed to fly for a given distance is the maximum range velocity. Flying at maximum range equates to a 14% savings compared to flying the same distance at minimum power velocity. When it is considered that on average a commuting trip consists of 44% soaring behavior, there is a 35% energy reduction compared to flying at maximum range velocity, demonstrating an obvious potential benefit to flying slower than solely at the maximum range velocity. Furthermore, the shallow minima of the power curve encompasses the velocity ranges required for all wind directions with only a +6% increase in mechanical power from the minimum power requirement; even with this power increase accounted for, the energy savings would be 31%. These energy saving estimates only provide half the story, suitable for comparison of a flight where no soaring takes place with a flight where some percentage of soaring occurs. If the energy requirements of a flight with only soaring behavior is to be compared to a nonsoaring flight, a different method is required; the act of soaring requires no mechanical power input, but there is an inherent cost involved. Biologist have previously made comparisons by considering the ratios of energy above the basal metabolic rate (BMR) for different behaviors [36]. The BMR ratios for flapping and soaring flights have been set at seven and two times the BMR taken from [51,52], respectively. It is not clear within the literature whether the increase in mechanical power required to vary airspeed in flapping flight is analogous to an increase in physical effort, so we will compare flying at the minimum power velocity and assume zero wind such that this is also the ground speed. Assuming minimum power velocity is also more comparable to the typical soaring speed, whereas the maximum range velocity is much higher and would require a large amount of environment energy to achieve. In this case, the energetic savings that could be achieved in a fully soaring flight would be 71%; however, the estimate lacks details of the additional distance required in order to find and exploit environmental sources such as thermals. The costs associated with the powered and unpowered flight sections for an SUAV have different ratios. A conservative ratio was estimated using the current drawn logs from a University of Bristol Flight Lab modified Skywalker X8 [53,54] to be as much as 10:1 powered to unpowered, meaning the savings in a fully soaring flight could be as much as 90%. The issue with this estimate is that a flight with 100% soaring behavior was only seen in the gulls on days with thermals, where the overall flight time and distance would increase to account for the thermaling sections of

flight and would reduce the overall savings by some amount. On nonthermal days, the gulls were able to achieve an average of 44% soaring behavior, so perhaps this is a more realistic potential for SUAVs also using wind based soaring. However, even with the same flight mode averages, dual-flight capabilities could provide a significant 56% energy savings. Again, the figure does not take into account additional distance or variable speed required in order to locate and exploit environmental energy sources and so has to be taken as an overestimation.

Nevertheless, SUAVs could benefit from the same dual flight mode speed matching strategy, taking into account the best performance velocities during the design phase of the platform. Matching the minimum power and best glide velocities for a platform would result in efficient use of environmental energy while demanding the lowest mechanical power for a motor when environmental energy sources are unavailable. Additionally, the performance curves of the platforms should have wide shallow minima to facilitate velocity matching for a wide range of wind speeds and result in low sink speeds. The FAR regulations for a gull-sized platform resulted in relatively low maximum velocities; however, as SUAV platforms do not require the same wing-beat power demands as gulls, the aspect ratio could be increased, further reducing mechanical power demand.

Applying the optimized airspeed adjustments on SUAVs requires information regarding the heading trajectory and the wind conditions. Current onboard sensors record airspeed and trajectory heading; however, the surrounding wind conditions are not normally measured. There have been recent developments regarding flow sensing in flight, where the wind conditions can be calculated using differential airspeed sensors [55], distributed pressure sensors [56], and estimated by tracking the drift of the vehicle when circling [57]. As these techniques continue to improve, airspeed matching that facilitates energy harvesting may become more commonplace, too. Current energy harvesting methods focus on locating updrafts; however, platforms in the future, such those designed for smart cities [58,59], may need to follow strict trajectories. The methods used by the gulls suggests that energy harvesting can often be achieved without having to deviate significantly from a direct flight path and that by being aware of the wind field there are considerable opportunities for energy savings when flying in urban environments.

VI. Conclusions

Nine major conclusions can be taken from this study:

1) Urban nesting gulls demonstrated that there is extensive environmental energy available in the urban environment, as shown by the high percentage of soaring flight during their daily commutes.

2) Thermaling is a good strategy in the right conditions, with tracks suggesting that thermals were so numerous in the city that it was not necessary for the birds to use every thermal or deviate significantly from the shortest path.

3) The gulls thermaled slightly faster than their minimum sink speed, in what may be a tradeoff between maximum energy gains and stall avoidance.

4) The interthermaling velocities of the gulls were not fully explained by COT or STF models, which suggests that both energy and time could be drivers in velocity selection.

5) High levels of nonflapping flight were performed on days with low thermal availability through the combined use of orographic soaring and gliding.

6) The gulls flew at their best glide velocity during orographic soaring, making adjustments to fly faster in headwinds and slower in updrafts.

7) The gulls' minimum power speed in flapping flight is close to their best glide velocity in soaring. This means the gulls can switch easily between flapping and soaring as updrafts are discovered, promoting maximum energy harvesting potential.

8) Adjusting for headwinds in flapping flight while maintaining a speed close to the best glide velocity requires a mechanical power increase of 6% but could result in energy savings of 31%.

9) COT optimization is suitable for use in the urban environment and should be considered in the platform design of SUAVs in order to improve flight endurance.

This study outlined energy harvesting soar strategies used by gulls making daily urban commutes during the breeding season. Through monitoring urban gulls, it was found that there is an abundance of environmental energy available within urban areas, which could reduce average energetic flight costs by almost a third. The results also highlighted the potential for SUAVs, where platforms with soaring capabilities operating in similar urban conditions could reduce flight costs by more than half. Current soar-mode SUAV technology tends to focus on harvesting from thermals; however, it

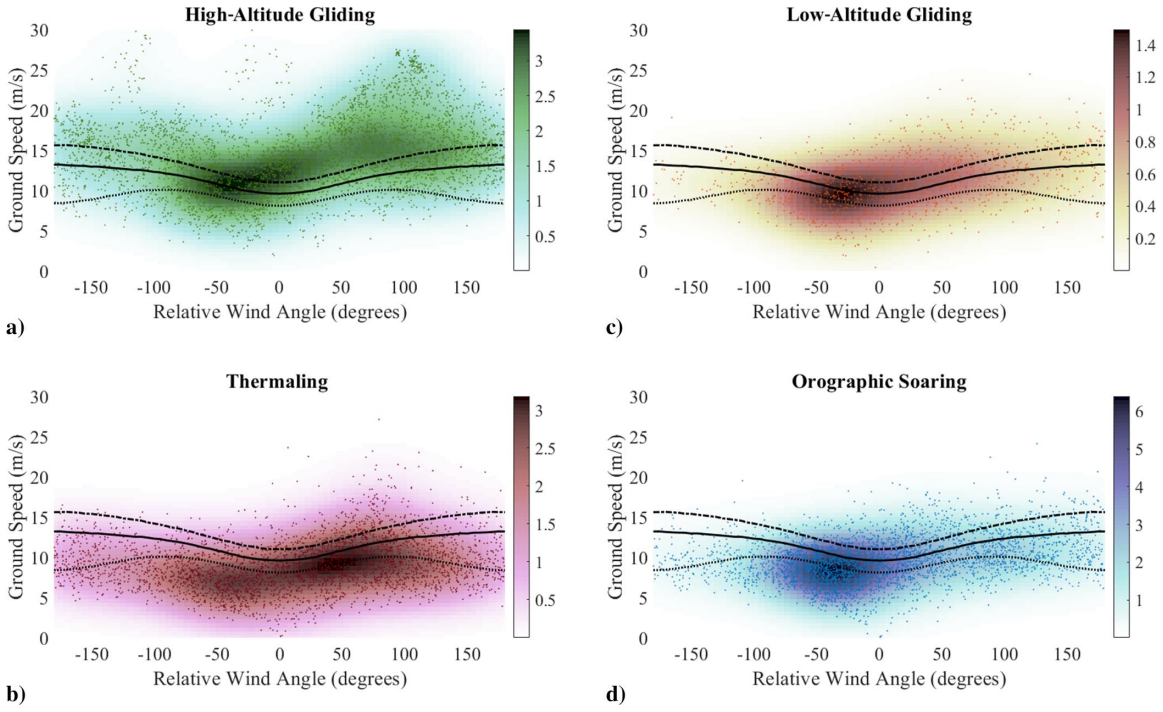

Fig. A1 Ground speed variation with the relative wind angle compared to COT for strategies a) high-altitude gliding, b) thermal soaring, c) low-altitude gliding, and d) orographic soaring.

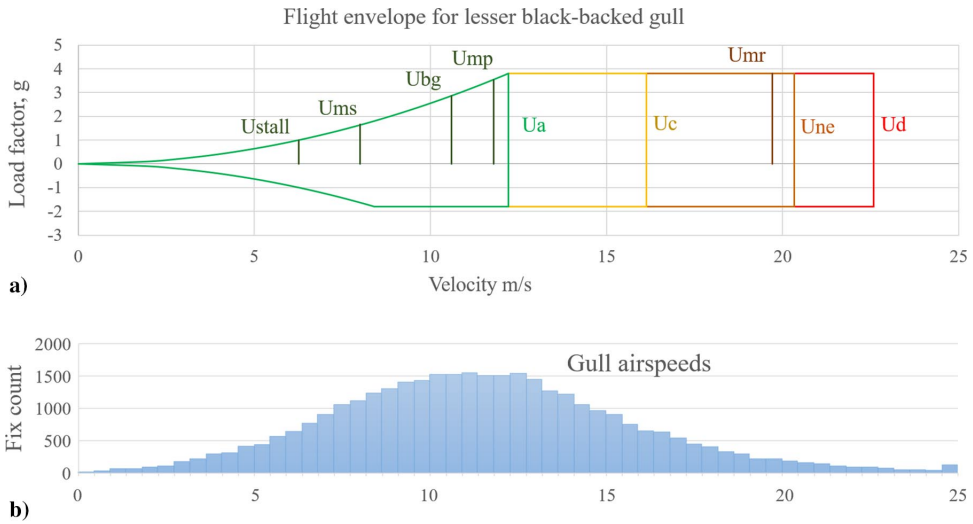

Fig. B1 a) Flight envelope for the average lesser black-backed gull using FAR regulations [50]. b) Histogram of airspeeds recorded in this study.

was found that the urban landscape also facilitates orographic soaring, meaning flight costs can also be reduced on days with little or no thermal sources. Furthermore, these findings provide bio-inspiration for the design of SUAV systems with dual flight-mode capabilities by outlining the importance of matching optimal velocities in order to maximize energy savings.

Appendix A: Ground Speeds

The soaring strategy velocity responses for wind direction were also calculated in the ground speed frame in order to demonstrate that the results were not caused by false correlation from using the wind data set in both the measured and modeled data. The ground speed models shown in Fig. A1 agree with the airspeed results from Sec. V.C, showing a trend of flying faster in high-altitude interthermal flight and slower in strategies which take advantage of updrafts.

All plots show resulting ground speed from the optimized airspeed using COT modeling with the horizontal wind, and the central line indicates no vertical wind. Upper and lower lines show a downdraft and updraft, respectively, both of 0.5 m/s strength. A Gaussian smoothing filter of 5σ was applied to the GPS fixes to demonstrate density.

Additionally, the Pearson R correlation coefficients were calculated for the measured velocity responses compared to model data generated using 1) measured wind data and 2) a randomized sample from the same wind data population. The tests were performed for flapping flight and orographic and low-altitude gliding flight combined. In both cases, there was no correlation between the model and the measured data when the model was generated using a random sample and a relatively high correlation between the model and measured data when the model was generated using measured wind data. Results are as follows: flapping flight ($R = 0.6$, RMSE $= 3.12$, $n > 10{,}000$, $p < 0.001$), flapping flight randomized sample ($R = 0.004$, RMSE $=$ 4.88, $n > 10{,}000$, $p < 0.001$), orographic and low-altitude flight combined ($R = 0.65$, RMSE $= 3.41$, $n > 10{,}000$, $p < 0.001$), and orographic and low-altitude flight randomized sample ($R = -0.01$, RMSE $= 5.39$, $n > 10{,}000$, $p < 0.001$).

Appendix B: Flight Envelope

The flight envelope of a lesser black-backed gull (Fig. B1a) was calculated using the size characteristics of the average lesser black-backed gull and the FAR regulations regarding wing loading [50]. A flight envelope charts the velocity versus the load factor and shows the performance safety limits of an aircraft. The important velocities in the flight envelope are the stall speed U_{stall}, maneuvre speed U_a, cruise speed U_c, never exceed or maximum operating speed U_ne, and finally the maximum dive speed U_d. Normal flight operation occurs between U_a and U_c. The velocities from the performance curves were also added. These are labeled as minimum sink velocity U_{ms}, best glide velocity U_{bg}, minimum power velocity U_{mp}, and maximum range velocity U_{mr}. Interestingly, the performance velocities are all in the slower region of the flight envelope and contain the majority of the recorded airspeeds, as shown in the histogram in Fig. B1b.

Acknowledgments

This project has received funding from the European Research Council under the European Union's Horizon 2020 research and innovation programme (grant agreement 679355) and was partially supported by the EPSRC Centre for Doctoral Training in Future Autonomous and Robotic Systems at the Bristol Robotics Laboratory.

References

[1] Cai, G., Dias, J., and Seneviratne, L., "A Survey of Small-Scale Unmanned Aerial Vehicles: Recent Advances and Future Development Trends," *Unmanned Systems*, Vol. 2, No. 2, 2014, pp. 175–199. https://doi.org/10.1142/S2301385014300017

[2] Girard, A. R., Howell, A. S., and Hedrick, J. K., "Border Patrol and Surveillance Missions Using Multiple Unmanned Air Vehicles," *2004 43rd IEEE Conference on Decision and Control (CDC) (IEEE Cat. No. 04CH37601)*, Vol. 1, Inst. of Electrical and Electronics Engineers, New York, 2004, pp. 620–625. https://doi.org/10.1109/CDC.2004.1428713

[3] Tomic, T., Schmid, K., Lutz, P., Domel, A., Kassecker, M., Mair, E., Grixa, I. L., Ruess, F., Suppa, M., and Burschka, D., "Toward a Fully Autonomous UAV: Research Platform for Indoor and Outdoor Urban Search and Rescue," *IEEE Robotics & Automation Magazine*, Vol. 19, No. 3, 2012, pp. 46–56. https://doi.org/10.1109/MRA.2012.2206473

[4] Thiels, C. A., Aho, J. M., Zietlow, S. P., and Jenkins, D. H., "Use of Unmanned Aerial Vehicles for Medical Product Transport," *Air Medical Journal*, Vol. 34, No. 2, 2015, pp. 104–108. https://doi.org/10.1016/j.amj.2014.10.011

[5] Murray, C. C., and Chu, A. G., "The Flying Sidekick Traveling Salesman Problem: Optimization of Drone-Assisted Parcel Delivery," *Transportation Research Part C: Emerging Technologies*, Vol. 54, May 2015, pp. 86–109. https://doi.org/10.1016/j.trc.2015.03.005

[6] Watkins, S., Milbank, J., Loxton, B. J., and Melbourne, W. H., "Atmospheric Winds and Their Implications for Microair Vehicles," *AIAA Journal*, Vol. 44, No. 11, 2006, pp. 2591–2600. https://doi.org/10.2514/1.22670

[7] Watkins, S., Thompson, M., Loxton, B., and Abdulrahim, M., "On Low Altitude Flight Through the Atmospheric Boundary Layer," *International Journal of Micro Air Vehicles*, Vol. 2, No. 2, 2010, pp. 55–68. https://doi.org/10.1260/1756-8293.2.2.55

[8] Watkins, S., Fisher, A., Mohamed, A., Marino, M., Thompson, M., Clothier, R., and Ravi, S., "The Turbulent Flight Environment Close to

the Ground and its Effects on Fixed and Flapping Wings at Low Reynolds Number," *5th European Conference for Aeronautics and Space Sciences*, 2013.

[9] Bronz, M., Moschetta, J. M., Brisset, P., and Gorraz, M., "Towards a Long Endurance MAV," *International Journal of Micro Air Vehicles*, Vol. 1, No. 4, 2009, pp. 241–254. https://doi.org/10.1260/175682909790291483

[10] Gavrilovic, N., Mohamed, A., Marino, M., Watkins, S., Moschetta, J.-M., and Bénard, E., "Avian-Inspired Energy-Harvesting from Atmospheric Phenomena for Small UAVs," *Bioinspiration & Biomimetics*, Vol. 14, No. 1, 2018, Paper 016006. https://doi.org/10.1088/1748-3190/aaec61

[11] Spelt, A., Williamson, C., Shamoun-Baranes, J., Shepard, E., Rock, P., and Windsor, S., "Habitat Use of Urban-Nesting Lesser Black-Backed Gulls During the Breeding Season," *Scientific Reports*, Vol. 9, No. 1, 2019, pp. 1–11. https://doi.org/10.1038/s41598-019-46890-6

[12] Klaassen, R. H., Ens, B. J., Shamoun-Baranes, J., Exo, K.-M., and Bairlein, F., "Migration Strategy of a Flight Generalist, the Lesser Black-Backed Gull Larus Fuscus," *Behavioral Ecology*, Vol. 23, No. 1, 2012, pp. 58–68. https://doi.org/10.1093/beheco/arr150

[13] McLaren, J. D., Shamoun-Baranes, J., Camphuysen, C., and Bouten, W., "Directed Flight and Optimal Airspeeds: Homeward-Bound Gulls React Flexibly to Wind Yet Fly Slower than Predicted," *Journal of Avian Biology*, Vol. 47, No. 4, 2016, pp. 476–490. https://doi.org/10.1111/jav.00828

[14] Shepard, E. L. C., Williamson, C., and Windsor, S. P., "Fine-Scale Flight Strategies of Gulls in Urban Airflows Indicate Risk and Reward in City Living," *Philosophical Transactions of the Royal Society B: Biological Sciences*, Vol. 371, No. 1704, 2016, Paper 20150394. https://doi.org/10.1098/rstb.2015.0394

[15] Guerra-Langan, A., Araujo-Estrada, S., and Windsor, S., "UAV Control Costs Mirror Bird Behaviour When Soaring Close to Buildings," *11th International Micro Air Vehicle Competition and Conference*, 2019.

[16] White, C., Watkins, S., Lim, E., and Massey, K., "The Soaring Potential of a Micro Air Vehicle in an Urban Environment," *International Journal of Micro Air Vehicles*, Vol. 4, No. 1, 2012, pp. 1–13. https://doi.org/10.1260/1756-8293.4.1.1

[17] Pennycuick, C. J., "A Wind-Tunnel Study of Gliding Flight in the Pigeon Columba Livia," *Journal of Experimental Biology*, Vol. 49, No. 3, 1968, pp. 509–526.

[18] Dial, K., Biewener, A., Tobalske, B., and Warrick, D., "Mechanical Power Output of Bird Flight," *Nature (London)*, Vol. 390, No. 6655, 1997, pp. 67–70. https://doi.org/10.1038/36330

[19] Hedrick, T. L., Tobalske, B. W., and Biewener, A. A., "How Cockatiels (Nymphicus hollandicus) Modulate Pectoralis Power Output Across Flight Speeds," *Journal of Experimental Biology*, Vol. 206, No. 8, 2003, pp. 1363–1378. https://doi.org/10.1242/jeb.00272

[20] Tucker, V. A., and Parrott, G. C., "Aerodynamics of Gliding Flight in a Falcon and Other Birds," *Journal of Experimental Biology*, Vol. 52, No. 2, 1970, pp. 345–367.

[21] Pennycuick, C., Heine, C. E., Kirkpatrick, S. J., and Fuller, M. R., "The Profile Drag of a Hawk's Wing, Measured by Wake Sampling in a Wind Tunnel," *Journal of Experimental Biology*, Vol. 165, No. 1, 1992, pp. 1–19.

[22] Lentink, D., Müller, U., Stamhuis, E., De Kat, R., Van Gestel, W., Veldhuis, L., Henningsson, P., Hedenström, A., Videler, J. J., and Van Leeuwen, J. L., "How Swifts Control Their Glide Performance with Morphing Wings," *Nature (London)*, Vol. 446, No. 7139, 2007, p. 1082. https://doi.org/10.1038/nature05733

[23] Rosen, M., and Hedenstrom, A., "Gliding Flight in a Jackdaw: A Wind Tunnel Study," *Journal of Experimental Biology*, Vol. 204, No. 6, 2001, pp. 1153–1166.

[24] Alerstam, T., and Lindström, Å., "Optimal Bird Migration: The Relative Importance of Time, Energy, and Safety," *Bird Migration*, Springer-Verlag, Berlin, 1990, pp. 331–351. https://doi.org/10.1007/978-3-642-74542-3_22

[25] Åkesson, S., and Hedenström, A., "Wind Selectivity of Migratory Flight Departures in Birds," *Behavioral Ecology and Sociobiology*, Vol. 47, No. 3, 2000, pp. 140–144. https://doi.org/10.1007/s002650050004

[26] Alerstam, T., "Optimal Bird Migration Revisited," *Journal of Ornithology*, Vol. 152, No. S1, 2011, pp. 5–23. https://doi.org/10.1007/s10336-011-0694-1

[27] Pennycuick, C. J., *Modelling the Flying Bird*, Vol. 5, Elsevier, London, 2008.

[28] MacCready, P. B., "Optimum Airspeed Selector," *Soaring (January–February)*, Vol. 10, No. 11, 1958, p. 10.

[29] Lawrance, N. R., and Sukkarieh, S., "Autonomous Exploration of a Wind Field with a Gliding Aircraft," *Journal of Guidance, Control, and Dynamics*, Vol. 34, No. 3, 2011, pp. 719–733. https://doi.org/10.2514/1.52236

[30] Taylor, G. K., Reynolds, K. V., and Thomas, A. L., "Soaring Energetics and Glide Performance in a Moving Atmosphere," *Philosophical Transactions of the Royal Society B: Biological Sciences*, Vol. 371, No. 1704, 2016, Paper 20150398. https://doi.org/10.1098/rstb.2015.0398

[31] Hedrick, T. L., Pichot, C., and De Margerie, E., "Gliding for a Free Lunch: Biomechanics of Foraging Flight in Common Swifts (Apus apus)," *Journal of Experimental Biology*, Vol. 221, No. 22, 2018, Paper jeb186270. https://doi.org/10.1242/jeb.186270

[32] Pennycuick, C. J., "Thermal Soaring Compared in Three Dissimilar Tropical Bird Species, Fregata Magnificens, Pelecanus Occidentals and Coragyps Atratus," *Journal of Experimental Biology*, Vol. 102, No. 1, 1983, pp. 307–325.

[33] Pennycuick, C. J., "Field Observations of Thermals and Thermal Streets, and the Theory of Cross-Country Soaring Flight," *Journal of Avian Biology*, Vol. 29, No. 1, 1998, pp. 33–43. https://doi.org/10.2307/3677338

[34] Ákos, Z., Nagy, M., Leven, S., and Vicsek, T., "Thermal Soaring Flight of Birds and Unmanned Aerial Vehicles," *Bioinspiration & Biomimetics*, Vol. 5, No. 4, 2010, Paper 045003. https://doi.org/10.1088/1748-3182/5/4/045003

[35] Bouten, W., Baaij, E. W., Shamoun-Baranes, J., and Camphuysen, K. C., "A Flexible GPS Tracking System for Studying Bird Behaviour at Multiple Scales," *Journal of Ornithology*, Vol. 154, No. 2, 2013, pp. 571–580. https://doi.org/10.1007/s10336-012-0908-1

[36] Shamoun-Baranes, J., Bouten, W., van Loon, E. E., Meijer, C., and Camphuysen, C., "Flap or Soar? How a Flight Generalist Responds to Its Aerial Environment," *Philosophical Transactions of the Royal Society B: Biological Sciences*, Vol. 371, No. 1704, 2016, Paper 20150395. https://doi.org/10.1098/rstb.2015.0395

[37] Anon., "LIDAR Composite DEM," Environment Agency, Oct. 2019, https://ckan.publishing.service.gov.uk/dataset/lidar-composite-dtm-2017-2m [retrieved May 2020].

[38] "Unified Model," MetOffice, Nov. 2017, https://www.metoffice.gov.uk/research/modelling-systems/unified-model.

[39] Database Image SIO, U. N. N. G., NOAA, "5129'52.84"N,233' 20.72 W"," Oct. 2019, GOOGLE EARTH, Getmapping, 4.19.2018.

[40] Langelaan, J., "Biologically Inspired Flight Techniques for Small and Micro Unmanned Aerial Vehicles," *AIAA Guidance, Navigation and Control Conference and Exhibit*, AIAA Paper 2008-6511, 2008. https://doi.org/10.2514/6.2008-6511

[41] Bonnin, V., Bénard, E., Moschetta, J.-M., and Toomer, C. A., "Energy-Harvesting Mechanisms for UAV Flight by Dynamic Soaring," *International Journal of Micro Air Vehicles*, Vol. 7, No. 3, 2015, pp. 213–229. https://doi.org/10.1260/1756-8293.7.3.213

[42] Liu, D.-N., Hou, Z.-X., Guo, Z., Yang, X.-X., and Gao, X.-Z., "Bio-Inspired Energy-Harvesting Mechanisms and Patterns of Dynamic Soaring," *Bioinspiration & Biomimetics*, Vol. 12, No. 1, 2017, Paper 016014. https://doi.org/10.1088/1748-3190/aa547c

[43] Taha, H., "Urban Climates and Heat Islands: Albedo, Evapotranspiration, and Anthropogenic Heat," *Energy and Buildings*, Vol. 25, No. 2, 1997, pp. 99–103. https://doi.org/10.1016/S0378-7788(96)00999-1

[44] Stone, B., Jr., and Rodgers, M. O., "Urban Form and Thermal Efficiency: How the Design of Cities Influences the Urban Heat Island Effect," *American Planning Association. Journal of the American Planning Association*, Vol. 67, No. 2, 2001, pp. 186–198. https://doi.org/10.1080/01944360108976228

[45] Eshelby, M., *Aircraft Performance: Theory and Practice*, AIAA, Reston, VA, 2000, Chap. 4.

[46] Welch, A., Irving, F., and Welch, L., *New Soaring Pilot*, Murray, London, 1977, Chap. 7.

[47] Pennycuick, C., "The Soaring Flight of Vultures," *Scientific American*, Vol. 229, No. 6, 1973, pp. 102–109. https://doi.org/10.1038/scientificamerican1273-102.

[48] Piggott, D., *Understanding Gliding: The Principles of Soaring Flight*, Barnes & Noble, New York, 1977, Chap. 3.

[49] Makovkin, D., and Langelaan, J. W., "Optimal Persistent Surveillance Using Coordinated Soaring," *AIAA Guidance, Navigation, and Control*

Conference, AIAA Paper 2014-0261, 2014.
https://doi.org/10.2514/6.2014-0261

[50] "FAA (Federal Aviation Administration) Airworthiness Standards: FAR Part 23: Normal, Utility, Acrobatic and Commuter Category Airplanes," July 2009.

[51] Tucker, V. A., "Metabolism During Flight in the Laughing Gull, Larus Atricilla," *American Journal of Physiology-Legacy Content*, Vol. 222, No. 2, 1972, pp. 237–245.
https://doi.org/10.1152/ajplegacy.1972.222.2.237.

[52] Baudinette, R., and Schmidt-Nielsen, K., "Energy Cost of Gliding Flight in Herring Gulls," *Nature (London)*, Vol. 248, No. 5443, 1974, pp. 83–84.
https://doi.org/10.1038/248083b0

[53] Schellenberg, B., Richardson, T., Watson, M., Greatwood, C., Clarke, R., Thomas, R., Wood, K., Freer, J., Thomas, H., Liu, E., and Salama, F., "Remote Sensing and Identification of Volcanic Plumes Using Fixed-Wing UAVs over Volcán de Fuego, Guatemala," *Journal of Field Robotics*, Vol. 36, No. 7, 2019, pp. 1192–1211.
https://doi.org/10.1002/rob.21896

[54] Schellenberg, B., Richardson, T. S., Clarke, R. J., Watson, M., Freer, J., McConville, A., and Chigna, G., "BVLOS Operations of Fixed-Wing UAVs for the Collection of Volcanic Ash Above Fuego Volcano, Guatemala," *AIAA Scitech 2020 Forum*, AIAA Paper 2020-2204, 2020.
https://doi.org/10.2514/6.2020-2204

[55] Mohamed, A., Abdulrahim, M., Watkins, S., and Clothier, R., "Development and Flight Testing of a Turbulence Mitigation System for Micro Air Vehicles," *Journal of Field Robotics*, Vol. 33, No. 5, 2016, pp. 639–660.
https://doi.org/10.1002/rob.21626

[56] Araujo-Estrada, S. A., Salama, F., Greatwood, C. M., Wood, K. T., Richardson, T. S., and Windsor, S. P., "Bio-Inspired Distributed Strain and Airflow Sensing for Small Unmanned Air Vehicle Flight Control," *AIAA Guidance, Navigation, and Control Conference*, AIAA Paper 2017-1487, 2017.
https://doi.org/10.2514/6.2017-1487

[57] Callou, F., and Foinet, G., U.S. Patent Application for "Method for Controlling a Multi-Rotor Rotary-Wing Drone, with Cross Wind and Accelerometer Bias Estimation and Compensation," Docket No. 9,488,978, filed 27 March 2013.

[58] Mohammed, F., Idries, A., Mohamed, N., Al-Jaroodi, J., and Jawhar, I., "UAVs for Smart Cities: Opportunities and Challenges," *2014 International Conference on Unmanned Aircraft Systems (ICUAS)*, Inst. of Electrical and Electronics Engineers, New York, 2014, pp. 267–273.
https://doi.org/10.1109/ICUAS.2014.6842265

[59] Menouar, H., Guvenc, I., Akkaya, K., Uluagac, A. S., Kadri, A., and Tuncer, A., "UAV-Enabled Intelligent Transportation Systems for the Smart City: Applications and Challenges," *IEEE Communications Magazine*, Vol. 55, No. 3, 2017, pp. 22–28.
https://doi.org/10.1109/MCOM.2017.1600238 CM

H. Dong
Associate Editor